

Extended Strong Tracking Filter SLAM Algorithm

Feng Wen, Xiaojie Chai, Yuan Li, Wei Zou and Kui Yuan

*Institute of Automation
 Chinese Academy of Sciences*

95 Zhongguancun East Road, 100190, Beijing, CHINA

{feng.wen, xiaojie.chai, yuan.li, wei.zou, kui.yuan}@ia.ac.cn

Abstract - Simultaneous Localization and Mapping (SLAM) is a key issue in robotics community. This paper presents a monocular vision and odometer based SLAM algorithm, making use of a novel artificial landmark which is called MR (Mobile Robot) code. During robot motion, the information from visual observations is fused with that from the odometer by Extended Strong Tracking Filter (STF), which can construct highly accurate maps and locate the robot more accurately than EKF. A new calculation method of suboptimal multiple fading factors is proposed which overcomes the problem of discontinuous observation in normal STF SLAM. Actual experiments are carried out in indoor environment, which shows that the proposed algorithm has improved the localization precision of the robot and the map accuracy.

Index Terms – mobile robot, SLAM, strong tracking filter, artificial landmark.

I. INTRODUCTION

Simultaneous Localization and Mapping (SLAM) is considered as the key issue in implementation of autonomous robot because of the important theoretic value and application prospect. The basic solution to SLAM algorithm was proposed by Smith and Cheeseman [1], which used Extended Kalman Filter (EKF). After that, many solutions were proposed to improve the basic solutions in many aspects.

In EKF SLAM, it always needs to compute the Jacobian matrix and only gets the first order of the Taylor expanded equation of the nonlinear system. If the predicted states don't approximate to the true states, it will result in large linearization errors. On the basis of orthogonality principle, Strong Tracking Filter (STF) is proposed by Zhou Donghua by introducing time-varying fading factor and selecting a suitable time-varying filter gain matrix online to guarantee orthogonality or approximate orthogonality of the error, thus can strongly increase the state estimation precision [2].

Some researchers have already applied STF in SLAM called STF SLAM. Zeng Jing employed a suboptimal fading factor $\lambda(k)$ to adapt Kalman gain online [3], while Huiping Li employed suboptimal multiple fading factors $\Lambda(k)$ [4]. But neither of the algorithms applies to the situations of discontinuous observation, which are common in practical applications of SLAM, nor discusses the effect of fading factors on state covariance.

In this paper, an extended multiple fading strong tracking filter SLAM algorithm is proposed and the calculation method of the multiple fading factors is also described. The algorithm is able to decrease the error induced by the linearization,

improve the localization precision and the map accuracy and constrain the covariance within a small range to enhance the credibility of the map.

The following part of this paper is organized as follows. The outline of Strong Tracking Filer is presented in Section II. After introducing MR code system, section III describes the motion model and observation model. The process and implementation of extended STF SLAM algorithm is put forward in section IV. In section V, actual experiments using the MR code are carried out, comparison and analysis of normal STF SLAM and extended STF SLAM are given, which shows the effectiveness of the proposed method. Some discussions are given in section VI.

II. STRONG TRACKING FILTER

Consider the following discrete nonlinear system:

$$\begin{aligned} x(k+1) &= f(u(k), x(k)) + \Gamma(k) \cdot v(k) \\ y(k+1) &= h(x(k+1)) + e(k+1) \end{aligned} \quad (1)$$

where the state vector $x(k) \in R^n$, the input vector $u(k) \in R^m$, the output vector $y(k) \in R^m$, and the nonlinear functions $f: R^m \times R^n \rightarrow R^n$, $h: R^n \rightarrow R^m$ have continuous partial derivative with regard to x ; process noise $v(k) \in R^q$ and measurement noise $e(k) \in R^m$ are Gaussian white noises with covariance $Q(k)$ and $R(k)$, respectively. $\Gamma(k)$ is a known matrix with appropriate dimension.

There exists the following Strong Tracking Filter [2]:

$$\hat{x}(k+1|k+1) = \hat{x}(k+1|k) + K(k+1) \cdot \gamma(k+1) \quad (2)$$

$$\hat{x}(k+1|k) = f(u(k), \dot{x}(k|k)) \quad (3)$$

The Strong Tracking Filter has the following good properties: lower sensitivity to the statistics of the initial states and the statistics of the system and /or measurement noise; stronger tracking ability to the suddenly changing states no matter whether the filter operates in dynamic or stationary fashion; acceptable computational complexity.

The above STF is deduced by introducing multiple sub-optimal fading factors into the prediction error covariance equation of the EKF. The sub-optimal fading factors may be determined analytically by solving the following equations:

$$E\{[x(k+1) - \hat{x}(k+1|k+1)] \\ \cdot [x(k+1) - \hat{x}(k+1|k+1)]^T\} = \min \quad (4)$$

$$E[\gamma^T(k+1) \cdot \gamma(k+1+j)] = 0; \quad (j=1,2,\dots) \quad (5)$$

Equation (5) is called orthogonality principle, whose physical meaning is that the residual error series should be made orthogonal to each other at each step, so that all the useful information in the residual error series could be extracted.

III. MR CODE SYSTEM AND MODELS

A. MR code system

The shape of the MR code is designed to be an equilateral pentagon, and binary BCH code is adopted for our MR code system, which is a kind of linear circular block code and has powerful correcting ability [5]. MR code system can represent enough different locations, objects, etc., and has invariant characteristics under different viewing angles and illumination conditions.

Fig. 1(a) shows a prototype of MR code with 8×8 unit modules. The unit module on top of the MR code is used to denote the direction of the MR code, which is very helpful for the self-localization and navigation for mobile robot.

Detection-recognition algorithm of MR code was proposed in our previous work [6]. Fig. 1(b) is a picture selected from one of our experiments to demonstrate the effectiveness of the proposed detection algorithm.

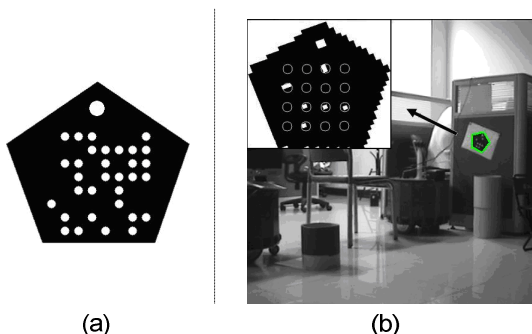


Fig. 1 (a)A prototype of MR code; (b) Detection and recognition.

Since the MR code can be printed on a paper and attached easily to places like ceilings, walls, etc., a mobile robot can identify its location or recognize an object using its vision system by simply recognizing the information represented by the MR code. Using the five vertexes of the extracted outline, the pose of the MR code relative to mobile robot can also be obtained. The details of the pose estimating methods can be found in our previous work [6].

B. Symbols

The state vector is defined as the pose of the robot and the locations of the landmarks which are observed.

$$X(k) = [X_r(k) \quad m_1 \quad \cdots \quad m_n]^T = \begin{bmatrix} X_r(k) \\ m \end{bmatrix} \quad (6)$$

At a time instant k , the following quantities are defined:

$X_r(k)$: The state vector describing the location and

orientation of the robot.

$u(k)$: The control vector, applied at time $k-1$ to drive the robot to a state $X_r(k)$ at the time k .

m_i : A vector describing the location of the i^{th} landmark whose true location is assumed time invariant.

$m = \{m_1, m_2, \dots, m_n\}$: The set of all landmarks.

$z_i(k)$: An observation taken from the robot of the location of the i^{th} landmark at time k .

$X_{0:k} = \{X(0), X(1), \dots, X(k)\}$: The history of robot locations.

C. Motion Model

Based on the assumption that an indoor mobile robot navigates on a flat floor, it is feasible to describe this problem in a 2-D frame. When the world coordinate frame $O_W X_W Y_W$ is defined, the pose of the robot is denoted by $X_r = [x_r, y_r, \theta_r]^T$, and θ_r denotes the angle from the direction of the robot to X_W within the range $(-\pi, \pi]$.

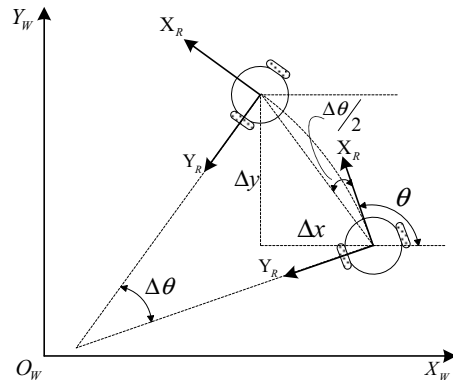


Fig. 2 Motion model.

For a differential-drive robot with an instruction cycle Δt , its movement can be analyzed as Fig. 2. When the robot moves from $X_r(k-1) = [x_r(k-1), y_r(k-1), \theta_r(k-1)]^T$ to $X_r(k) = [x_r(k), y_r(k), \theta_r(k)]^T$, the travelled distance is denoted by Δs and the angle $\Delta\theta$.

The odometric model takes $u(k) = [\Delta s(k), \Delta\theta(k)]^T$ as input data and can be represented as follows:

$$X_r(k) = f(X_r(k-1), u(k)) + w(k) \quad (7)$$

$w(k)$ is Gaussian white noises with covariance $Q(k)$. The error model for odometric position estimation can be found in

our previous work [7], in which $Q(k)$ is determined through actual experiments.

D. Observation Model

An observation taken from the robot of the location of the i^{th} landmark at time k is denoted as:

$$z_i(k) = [x_{i|s}(k), y_{i|s}(k), \theta_{i|s}(k)]^T \quad (8)$$

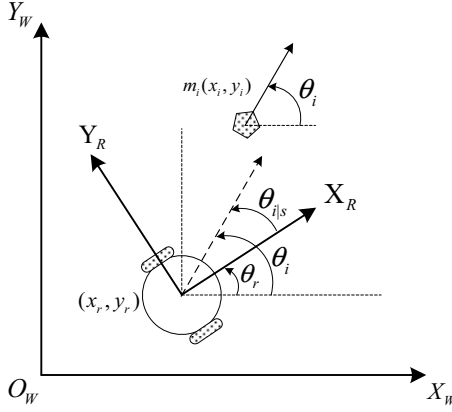


Fig. 3 Observation model.

$\theta_{i|s}$ represents the angle from the direction of the robot to the direction of the MR code as shown in Fig. 3. The camera is placed at the centre of robot. The observation model can be described as follows:

$$\begin{aligned} z_i(k) &= \begin{bmatrix} x_{i|s}(k) \\ y_{i|s}(k) \\ \theta_{i|s}(k) \end{bmatrix} = h(X(k)) + v(k) \\ &= \begin{bmatrix} \cos(\theta_r(k)) & \sin(\theta_r(k)) & 0 \\ -\sin(\theta_r(k)) & \cos(\theta_r(k)) & 0 \\ 0 & 0 & 1 \end{bmatrix} \begin{bmatrix} x_i - x_r(k) \\ y_i - y_r(k) \\ \theta_i - \theta_r(k) \end{bmatrix} + v(k) \end{aligned} \quad (9)$$

Measurement noise $v(k)$ is Gaussian white noise with covariance $R(k)$. The error model for Measurement estimation can be found in our previous work [7], in which $R(k)$ is determined through actual experiments.

IV. EXTENDED STF SLAM

A. Outline of the Algorithm

In practice the landmarks such as MR code can not be observed continuously. When the landmarks are out of the view of the robot, the time-update step of standard EKF SLAM is carried out. When landmarks are in sight, STF prediction, observation-update and initialization steps are taken. The process is shown in Fig. 4.

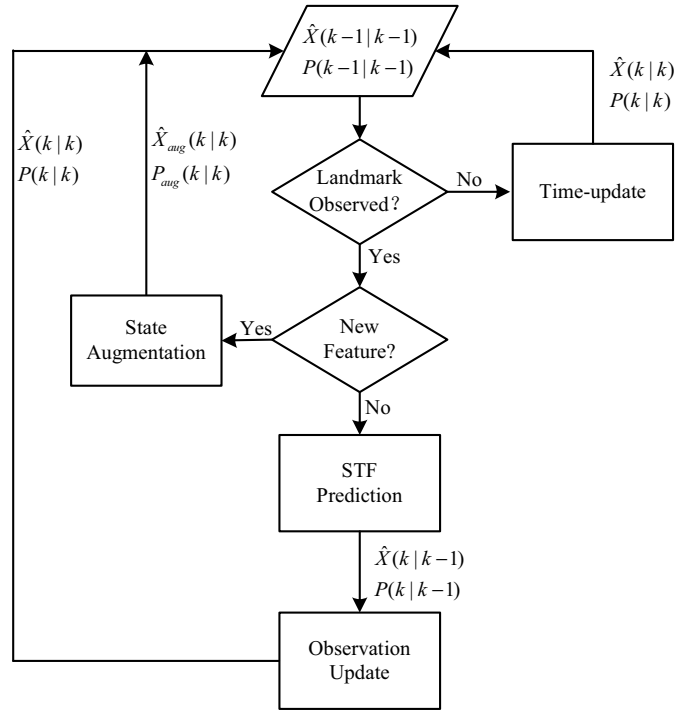


Fig. 4 Process of Extended STF SLAM.

B. Time-update

$$\hat{X}(k) = \begin{bmatrix} \hat{X}_r(k|k) \\ \hat{m}(k) \end{bmatrix} = \begin{bmatrix} f(\hat{X}_r(k-1|k-1), u(k)) \\ \hat{m}(k-1) \end{bmatrix} \quad (10)$$

For convenience, combined state vector $X(k)$ is used which comprises robot pose and the map. The motion model described in [7] is utilized and the full motion model with noise is as follows

$$\begin{aligned} X(k) &= g(X(k-1), u(k)) + \varepsilon(k) \\ &= X(k-1) + J_r^T \begin{bmatrix} \Delta s \cos(\theta + \Delta\theta/2) \\ \Delta s \sin(\theta + \Delta\theta/2) \\ \Delta\theta \end{bmatrix} + N(0, J_r^T Q(k) J_r) \end{aligned} \quad (11)$$

where J_r is a matrix that maps the 3-dimensional state vector into a vector of dimension $3N+3$, and $J_r^T Q(k) J_r$ extends the covariance matrix to the dimension of the full state vector squared.

$$J_r = \begin{bmatrix} 1 & 0 & 0 & 0 & \cdots & 0 \\ 0 & 1 & 0 & 0 & \cdots & 0 \\ 0 & 0 & 1 & 0 & \underbrace{\cdots}_{3N} & 0 \end{bmatrix} \quad (12)$$

The motion function g is approximated using a first degree Taylor expansion.

$$\begin{aligned} g(X(k-1), u(k)) &\approx g(\hat{X}(k-1), u(k)) + \\ &G(k) \cdot (X(k-1) - \hat{X}(k-1)) \end{aligned} \quad (13)$$

where

$$G(k) = \frac{\partial g(X(k), u(k))}{\partial X(k)} \Big|_{\hat{X}(k|k-1), u(k)} \quad (14)$$

$$= I + J_r^T \cdot g_t \cdot J_r$$

$$g_t = \begin{bmatrix} 0 & 0 & -\Delta s(k) \sin(\hat{\theta}_r(k-1|k-1) + \Delta\theta(k)/2) \\ 0 & 0 & \Delta s(k) \cos(\hat{\theta}_r(k-1|k-1) + \Delta\theta(k)/2) \\ 0 & 0 & 0 \end{bmatrix} \quad (15)$$

with covariance $P(k|k)$ at time k :

$$P(k|k) = G(k)P(k-1|k-1)G^T(k) + J_r^T Q(k)J_r \quad (16)$$

C. STF Prediction

$$\hat{X}(k|k-1) = \hat{X}(k-1|k-1) +$$

$$J_r^T \begin{bmatrix} \Delta s(k) \cos(\hat{\theta}_r(k-1|k-1) + \Delta\theta(k)/2) \\ \Delta s(k) \sin(\hat{\theta}_r(k-1|k-1) + \Delta\theta(k)/2) \\ \Delta\theta(k) \end{bmatrix} \quad (17)$$

Huiping Li exploited the method in [2] to calculate the covariance of the prediction step as follows

$$P'(k|k-1) = \Lambda(k) \cdot G(k) \cdot P(k-1|k-1) \quad (18)$$

$$\cdot G^T(k) + J_r^T Q(k) J_r$$

where $\Lambda(k)$ is suboptimal multiple fading factors:

$$\Lambda(k) = \text{diag}[\lambda_1(k), \lambda_2(k), \dots, \lambda_n(k)]; \quad (19)$$

$$\lambda_i(k) \geq 1, i = 1, 2, \dots, n$$

When $\lambda_1, \dots, \lambda_n$ are not equal, $P'(k|k-1)$ is an asymmetric matrix which can not satisfy the definition of a covariance matrix, so that the Cholesky decomposition can not be used to reduce the computational complexity of matrix inversion, which is one of the most computationally expensive steps when solving the Kalman gain.

Comparing suboptimal fading factors $\lambda(k)$ [8] and suboptimal multiple fading factors $\Lambda(k)$, we can assume that $\lambda(k)$ is assigned to the main diagonal elements of $\Lambda(k)$ according to a certain proportion. When $\lambda_1, \dots, \lambda_n$ are equal, the STF based on multiple fading factors deteriorates to a single fading factor based STF.

Here, new suboptimal multiple fading factors $T(k)$ are introduced in order that different variables of the state fade at different speed and covariance matrix is symmetric.

$$T(k) = \text{diag}[\tau_1(k), \dots, \tau_n(k)]; \quad (20)$$

$$\tau_i(k) = \sqrt{\lambda_i(k)}, i = 1, 2, \dots, n$$

where λ_i is identical with the variable in (19).

The covariance matrix in STF prediction is defined as:

$$P(k|k-1) = T(k) \cdot G(k) \cdot P(k-1|k-1) \quad (21)$$

$$\cdot G(k)^T \cdot T(k) + J_r^T Q(k) J_r$$

When i^{th} landmark is observed, the observation model in (9) is used. It is assumed that the i^{th} landmark observed at time k correspond to the j^{th} landmark stored in the map, thus:

$$z_i(k) = \begin{bmatrix} x_{j|s}(k) \\ y_{j|s}(k) \\ \theta_{j|s}(k) \end{bmatrix} = h(X(k)) + v(k) \quad (22)$$

$$= \begin{bmatrix} \cos(\theta_r(k)) & \sin(\theta_r(k)) & 0 \\ -\sin(\theta_r(k)) & \cos(\theta_r(k)) & 0 \\ 0 & 0 & 1 \end{bmatrix} \begin{bmatrix} x_j - x_r(k) \\ y_j - y_r(k) \\ \theta_j - \theta_r(k) \end{bmatrix} + N(0, R(k))$$

The observation function h is approximated using a first degree Taylor expansion.

$$h(X(k|k-1)) \approx h(\hat{X}(k|k-1)) \quad (23)$$

$$+ H_k^i(X(k|k-1) - \hat{X}(k|k-1))$$

where H_k^i is the partial derivative of h with the whole state $X(k|k-1)$.

In practice, STF employs one-step approximation to solve $\Lambda(k)$ online:

$$\Lambda(k) = \text{diag}\{\lambda_1(k), \lambda_2(k), \dots, \lambda_n(k)\} \quad (24)$$

$$\lambda_i(k) = \begin{cases} \alpha_i \eta(k); \alpha_i \eta(k) > 1 \\ 1; \quad \alpha_i \eta(k) \leq 1, i = 1, 2, \dots, n. \end{cases} \quad (25)$$

$$\eta(k) = \text{tr}[N(k)] / (\sum_{i=1}^n \alpha_i \cdot M_{ii}(k)) \quad (26)$$

$$N(k) = V_0(k) - R(k) - H_k^i \cdot J_r \cdot Q(k) \cdot J_r^T \cdot (H_k^i)^T \quad (27)$$

$$M(k) = G(k) \cdot P(k-1|k-1) \cdot G^T(k) \cdot (H_k^i)^T \cdot H_k^i \quad (28)$$

$$V_0(k) = E[\gamma(k) \cdot \gamma^T(k)] \approx$$

$$\begin{cases} \gamma(1) \cdot \gamma^T(1); & k = 0 \\ [\rho \cdot V_0(k-1) + \gamma(k) \cdot \gamma^T(k)] / (1 + \rho); & k \geq 1 \end{cases} \quad (29)$$

where in (29), $\rho = 0.95$ is a forgetting factor, and $\alpha_i \geq 1$ in (25) and (26) are pre-selected coefficients. If we know a priori that x_i varies quickly, we can select a larger α_i to improve the tracking ability of the STF.

STF assumes that the observation is continuous. However, in practical SLAM application, discontinuous observation is very common, and the observation at a different time is related to different variables of the state. Furthermore, the state dimension also varies with time. So, fixed α_i is not applicable to the fact of SLAM, and dynamic setting is necessary instead.

When the i^{th} landmark is observed, the current observation is only related to the robot pose and the state of the i^{th} landmark, and the corresponding value of α should

be raised. In addition, because the angular error is relatively bigger, the angular weights should be raised. The calculation method of α is as follows:

$$\alpha^x : \alpha^y : \alpha^\theta = 1:1:p \quad (30)$$

$$\alpha_x^j = \alpha_y^j = 1; \alpha_\theta^j = p \quad (j=1,2,\dots,N; j \neq i) \quad (31)$$

$$\alpha_x^i + \alpha_y^i + \alpha_\theta^i = q \cdot \sum_{j=1, j \neq i}^N (\alpha_x^j + \alpha_y^j + \alpha_\theta^j) \quad (32)$$

$$\alpha_x^r + \alpha_y^r + \alpha_\theta^r = r \cdot \sum_{j=1, j \neq i}^N (\alpha_x^j + \alpha_y^j + \alpha_\theta^j) \quad (33)$$

where (30) specifies the proportion of three components of the state of the robot and the landmark, N is the number of the landmarks at present and α_x^j denotes the value of the component of the j^{th} landmark in the x direction. In experiments, considering the sensitivities of the components, a set of typical values is $p = 3; q = 1.25; r = 0.25$.

D. Observation Update

$$\hat{X}(k|k) = \hat{X}(k|k-1) + W_i(k) \cdot \gamma(k) \quad (34)$$

$$P(k|k) = P(k|k-1) - W_i(k) S_i(k) W_i(k)^T \quad (35)$$

where

$$S_i(k) = H_k^i \cdot P(k|k-1) \cdot (H_k^i)^T + R_i(k) \quad (36)$$

$$W_i(k) = P(k|k-1) \cdot (H_k^i)^T \cdot S_i(k)^{-1} \quad (37)$$

E. State Augmentation

When a landmark m_j is observed for the first time, we initialize the landmark estimate with the expected position, which is derived from the expected robot pose and the measurement variables for this landmark.

$$\hat{X}_{aug}(k|k) = \begin{bmatrix} \hat{X}(k|k-1) \\ \hat{m}_j(k) \end{bmatrix} \quad (38)$$

$$\hat{m}_j(k) = q(\hat{z}_i(k), \hat{X}_r(k|k-1)) \quad (39)$$

$$P_{aug}(k|k) = \begin{bmatrix} P_{rr}(k|k) & P_{rm}(k|k) & (P_{ar})^T \\ P_{mr}(k|k) & P_{mm}(k|k) & (P_{am})^T \\ P_{ar} & P_{am} & P_{aa} \end{bmatrix} \quad (40)$$

The newly added elements of $P_{aug}(k|k)$ are calculated as:

$$P_{aa} = \nabla_{X_r} q \cdot P_{rr} \cdot (\nabla_{X_r} q)^T + \nabla_{z_i} q \cdot R(k) \cdot (\nabla_{z_i} q)^T \quad (41)$$

$$P_{ar} = \nabla_{X_r} q \cdot P_{rr} \quad (42)$$

$$P_{am} = \nabla_{X_r} q \cdot P_{rm} \quad (43)$$

V. EXPERIMENTS

In order to validate our method, experiments were carried out using a mobile robot platform AIM developed in our lab as shown in Fig. 5. The mobile robot platform AIM is equipped with a Intel Centrino microprocessor clocked at 1600MHz, two wheel encoders, one color PTZ camera and 16 sonar sensors, etc..



Fig. 5 Experiment platform robot AIM.

The experiment is carried out in our lab. The scenario is shown in Fig. 6. Pentagons denote the MR codes which are attached to the dropped ceiling, and the solid line denotes the route of the robot. In order to facilitate comparison of experimental data, the robot starts from the location T1, travels along the route counterclockwise and repeats 3 circuits.

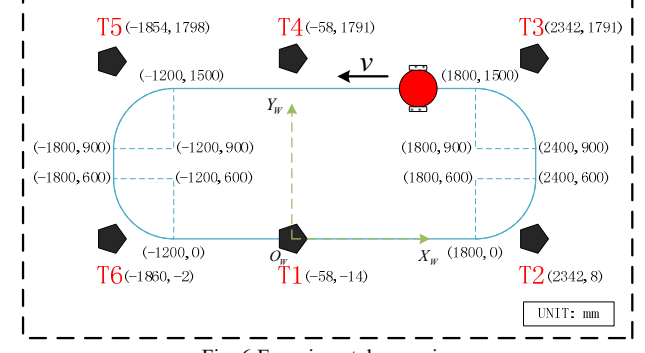


Fig. 6 Experimental scenario.

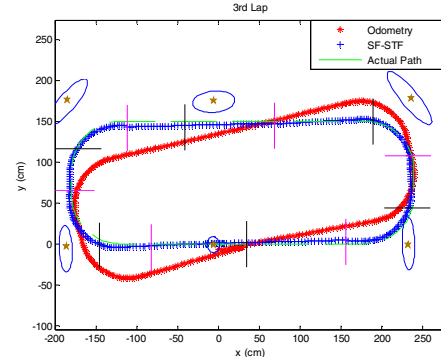


Fig. 7 SF-STFSLAM: the robot path with estimated landmark positions.

The experiment results are as shown in Fig. 7 and Fig. 8. The ellipses denote the 95% confidence bounds derived from estimated landmark location errors. Relative to SF-STFSLAM, the ellipses in EMF-STFLAM is obviously smaller, which means that the covariance is smaller and the credibility of the map is higher.

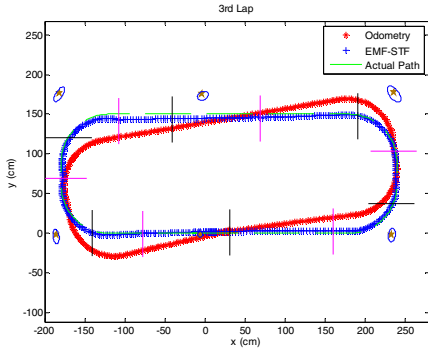


Fig. 8 EMF-STFSLAM: the robot path with estimated landmark positions.

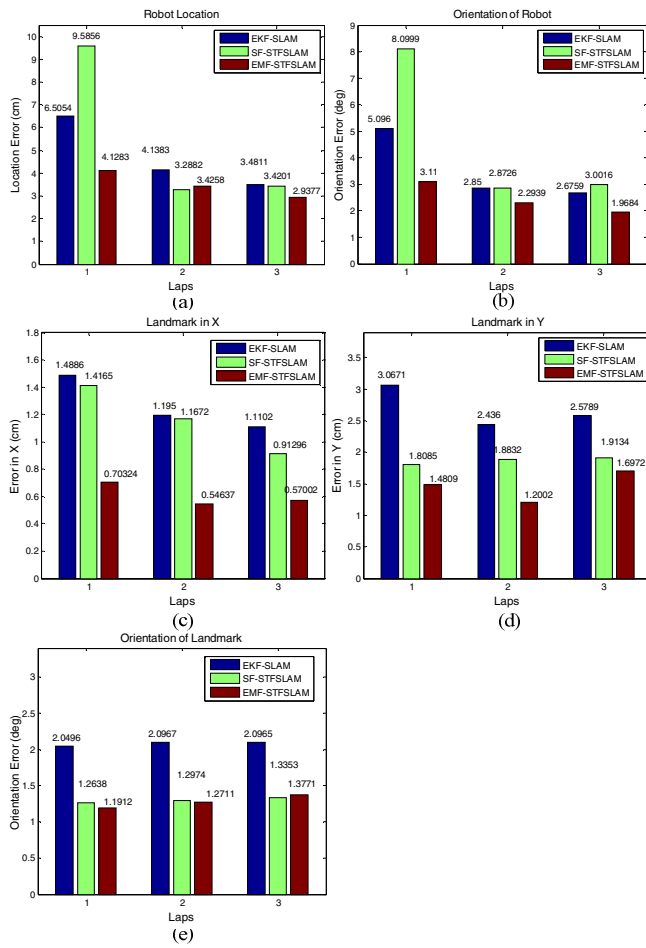


Fig. 9 Comparison of standard error of estimates.

Extended Multiple Fading STFSLAM (EMF-STFSLAM) was compared with Single Fading STFSLAM (SF-STFSLAM) and EKF-SLAM, and the comparison of the standard error of the state is shown in Fig. 9. At the aspects of the localization precision and the map accuracy, EMF-STFSLAM and SF-STFSLAM were superior to EKF-SLAM, and the superiority was more obvious in the map accuracy. As shown in Fig. 9(e), relative to EKF-SLAM, the estimation accuracy of landmarks' angle by both kinds of STFSLAM had

increased significantly, which showed the correction effect of fading factors on the angular estimate.

As shown in Fig. 9(a~d), EMF-STFSLAM was better than SF-STFSLAM on both localization precision and map accuracy. This is because that when the fading factor changed rapidly, SF-STFSLAM increased the covariance matrix of the whole state, which resulted in that all the state components excessively depended on the observation update; EMF-STFSLAM could dramatically increase the prediction covariance of the state components related to the current observed landmark, which resulted in that the estimate could rapidly track the changes of residual error and the correction weight of observation update to the estimate was increased. The variation scope of other state components was relatively smaller, which restrained the growth of the whole covariance, and kept the correction weight of odometric information to the estimate of other landmarks' state.

VI. CONCLUSIONS

In this paper, an extended multiple fading strong tracking filter SLAM algorithm is proposed and the calculation method of the multiple fading factors is also described. The algorithm is able to decrease the error induced by the linearization, improve the localization precision and the map accuracy and constrain the covariance within a small range to enhance the credibility of the map.

ACKNOWLEDGMENT

This work is supported by the National Natural Science Foundation of China (No. 60875051, No. 61075093) and National High Technology Research and Development Program of China (No. 2008AA040204, No. 2008AA040209, No. 2009AA043902-2).

REFERENCES

- [1] Smith, R. and P. Cheesman, "On the representation of spatial uncertainty," *Int. J. Robotics Research*, vol. 5, no. 4, pp. 56-68, 1987.
- [2] Zhou Donghua, et al, "A suboptimal multiple fading extended kalman filter," *Acta Automatica Sinica*, vol. 17, no. 6, pp. 599-695, Nov. 1991.
- [3] Zeng Jing, et al. "Study on Application of STF in Mobile Robot SLAM," in Proceedings of International Conference on Information Engineering and Computer Science, Wuhan, 2009, pp. 1-4.
- [4] Huiping, Li, et al, "Strong Tracking Filter Simultaneous Localization and Mapping Algorithm," in Proceedings of International Conference on Computer Science and Software Engineering, 2008, pp. 1085-1088.
- [5] Ranjan Bose, *Information theory coding and cryptography*, Simplified Chinese translation edition, Beijing: Chinese Machine Press, McGraw-Hill Education (Asia) Co., 2003, pp. 99.
- [6] Rui Zheng, Kui Yuan, "MR Code for Robot Self-localization," in Proceedings of 7th World Congress on Intelligent Control and Automation, 2008, pp. 7449-7454.
- [7] Wen Feng, et al, "A Visual SLAM Algorithm Based on a Novel Artificial Landmark System," in Proceedings of the 29th Chinese Control Conference, Beijing, China, July 29-31, 2010, pp. 3791-3797.
- [8] Zhou Donghua, et al, "Suboptimal Fading Extended Kalman Filter for Nonliner Systems," *Chinese J. Control and Decision*, vol. 5, pp. 1-6, 1990.